

# Rescuing Palindromic Universes with Improved Recombination Modelling

Metha Prathaban<sup>1,2</sup> and Will Handley<sup>1,3,4,\*</sup>

<sup>1</sup>*Astrophysics Group, Cavendish Laboratory, J.J. Thomson Avenue, Cambridge, CB3 0HE, UK*

<sup>2</sup>*Clare College, Trinity Lane, Cambridge, CB2 1TL, UK*

<sup>3</sup>*Kavli Institute for Cosmology, Madingley Road, Cambridge, CB3 0HA, UK*

<sup>4</sup>*Gonville & Caius College, Trinity Street, Cambridge, CB2 1TA, UK*

We explore the linearly quantised primordial power spectra associated with palindromic universes. Extending the results of Lasenby *et al.* [1] and Bartlett *et al.* [2], we improve the modelling of recombination and include higher orders in the photonic Boltzmann hierarchy. In so doing, we find that the predicted power spectra become largely consistent with observational data. The improved recombination modelling involves developing further techniques for dealing with the future conformal boundary, by integrating the associated perturbation equations both forwards and backwards in conformal time. The resulting wavevector quantisation gives a lowest allowed wavenumber  $k_0 = 9.93 \times 10^{-5} \text{Mpc}^{-1}$  and linear spacing  $\Delta k = 1.63 \times 10^{-4} \text{Mpc}^{-1}$ , providing fits consistent with observational data equivalent in quality to the  $\Lambda$ CDM model.

## I. INTRODUCTION

Astronomical observations [3, 4] have indicated that our current universe is in a state of acceleration, progressing towards an asymptotically de Sitter future; in conformal time, such a universe contains a cosmological coordinate horizon, referred to henceforth as the “Future Conformal Boundary” (FCB). Given that this so-called “end of the universe” occurs at a finite conformal time, the question thus arises as to what happens to physical quantities such as matter and radiation perturbations at the FCB itself and whether we can continue their development beyond this boundary. In fact, doing so has profound implications and consequences for the observational predictions made by perturbation theory, as demonstrated in previous work by several groups (Lasenby *et al.* [1], Bartlett *et al.* [2], Boyle and Turok [5]).

Lasenby *et al.* [1] have shown that perturbation variables remain non-singular at the FCB, and we are able to unambiguously continue them through this boundary. The answer as to what happens to perturbations beyond the FCB lies in considering how they approach the next genuine singularity, the so-called “Big Bang 2” (BB2). Since conformal time forms a “double cover” of the solutions, we should demand reflecting boundary conditions. Alternatively, since we are working to linear order in this treatment, we must require that our modes be finite everywhere. Thus we may only consider modes which are either symmetric or antisymmetric about the FCB to be valid, such that at BB2 they match onto the non-singular series from the first big bang (BB1). These symmetry conditions can also be interpreted as a “reflecting boundary condition” at the FCB, since conformal time forms a double cover of cosmic time.

From these symmetry conditions, we arrive at having only a discrete set of comoving wavenumbers,  $k$ , such

that the allowed modes undergo the correct number of cycles between BB1 and BB2. This is analogous to an infinite potential well in which boundary conditions lead to quantised solutions with a particular set of wavenumbers. This allowed set of wavenumbers has been analytically explored in Lasenby *et al.* [1] for flat- $\Lambda$  radiation-dominated and matter-dominated universes and numerically found for a concordance  $\Lambda$ CDM universe in Bartlett *et al.* [2].

Working with discrete comoving wavenumbers gives rise to a different Cosmic Microwave Background (CMB) power spectrum in comparison to the canonical calculation which uses a continuous set of  $k$ . We can, therefore, compute the predicted power spectra from the allowed wavenumbers and compare these to observational data [6], as shown in Fig. 1. The specific sets of  $k$  derived in previous work have been shown not to produce quantitatively good fits to current cosmological data, due to an unphysically large lowest allowed wavenumber,  $k_0$ ; however, it has been demonstrated that a linearly spaced set of  $k$  has the potential to provide significantly improved fits compared with the baseline concordance model of cosmology (Bartlett *et al.* [2]). Moreover, they are capable of qualitatively reproducing some of the interesting low-multipole features of the CMB power spectrum, which have generated much discussion and various potential explanations over the years [7–10]. Consequently, there are compelling reasons to investigate alternative quantised models which might predict these superior fits *a priori*.

In Lasenby *et al.* [1] and Bartlett *et al.* [2] post-recombination photons are treated as a fluid with anisotropic stress (termed “imperfect fluids”), which can be interpreted as including the first three terms in a photonic Boltzmann hierarchy. In this paper we build on this work by including the full photonic Boltzmann hierarchy. Making this extension requires a more sophisticated treatment of recombination modelling, whereby further free parameters are introduced via the exact values of higher order terms at the end of recombination; this enables us to have the correct number of degrees of freedom to satisfy the new quantisation conditions required within

\* wh260@mrao.cam.ac.uk

this model and obtain a more accurate set of  $k$  values. The first few allowed modes under this improved modelling of recombination are plotted for the base and some higher order variables in Figs. 2 and 3.

In Section II, we describe the background and perturbation equations we will be solving and present an overview of the work begun in Lasenby *et al.* [1] and Bartlett *et al.* [2]. We explain how to extend previous work to derive the new set of quantisation conditions necessary for these higher order terms and describe the modelling of recombination that has been used here in Section III. In Section IV the methods used to calculate the new set of allowed comoving wavenumbers within this model are described, with the results and its implications discussed in Section V. Finally, conclusions are presented in Section VI.

Throughout this paper we work in units of  $8\pi G = c = \hbar = 1$  and all overdots denote differentiation with respect to conformal time, unless otherwise explicitly stated.

## II. THEORETICAL BACKGROUND

### A. Cosmological Background Equation

For a homogeneous, isotropic and expanding universe, the most general metric is the Friedmann-Robertson-Walker (FRW) metric. Substituting this into the Einstein Field Equations and working within a perfect fluid approximation, we arrive at the background equation describing the evolution of such a universe:

$$\dot{s}^2 = H_0^2 \sum_i \Omega_{i,0} |s|^{3(1+w_i)}, \quad (1)$$

where  $s = \frac{1}{a}$  is the reciprocal scale factor,  $H_0$  is the present-day Hubble parameter value,  $\Omega_i$  is the  $i$ th fluid's dimensionless density parameter and  $w_i$  is the equation of state parameter for a given fluid  $i$  [2, 12]. Here, the subscripts  $r$ ,  $m$  and  $\Lambda$  are used to denote radiation, matter and the cosmological constant respectively. We use modulus signs in this case as  $s < 0$  when analytically continued beyond the FCB.

### B. Cosmological Perturbation Equations

#### 1. Perfect Fluid Approximation

We must now include perturbations to this background in our equations. The notation used in this section and in the rest of the paper largely follows [2, 13] and we work in the conformal Newtonian gauge.

If we assume that all components behave as perfect fluids, then it is possible to write the perturbation equations to linear order in matrix form, in a manner analogous to [14]:

$$\dot{\mathbf{x}} = M(\eta)\mathbf{x}; \quad (2)$$

$$\mathbf{x} = (\phi, \delta_r, \delta_m, v_r, v_m); \quad (3)$$

$$M = \begin{pmatrix} -\mathcal{H} & 0 & 0 & -2H_0^2\Omega_r s^2 & -\frac{3}{2}H_0^2\Omega_m |s| \\ -4\mathcal{H} & 0 & 0 & \frac{4}{3}k^2 - 8H_0^2\Omega_r s^2 & -6H_0^2\Omega_m |s| \\ -3\mathcal{H} & 0 & 0 & -6H_0^2\Omega_r s^2 & k^2 - \frac{9}{2}H_0^2\Omega_m |s| \\ -1 & -\frac{1}{4} & 0 & 0 & 0 \\ -1 & 0 & 0 & 0 & \mathcal{H} \end{pmatrix}, \quad (4)$$

where  $\mathcal{H} = \frac{\dot{a}}{a}$  is the conformal Hubble rate, perturbations to the background densities are denoted by  $\delta_i$ , the peculiar velocities of these perturbations are denoted by  $v_i$ , and  $\phi$  represents the Newtonian gauge potential [15].

#### 2. Higher Orders

After recombination, given the lack of free electrons available to scatter and isotropise the radiation, the evolution of the photon distribution can be expressed using  $F_\gamma(\vec{k}, \hat{n}, \tau)$ , and  $G_\gamma(\vec{k}, \hat{n}, \tau)$ , the sum and difference, respectively, of the phase space density of the two polarisation components of linearly polarised photons [13]. Following Lasenby *et al.* [1] and Bartlett *et al.* [2] we do not consider the  $G_{r\ell}$  terms further due to these decoupling from the rest of the equations once our approximation of free-streaming post-recombination is made, but unlike in Lasenby *et al.* [1] and Bartlett *et al.* [2] we do not assume  $F_{r\ell}$  to be zero for  $\ell > 2$

The matrix representation of the perturbation equations within this Boltzmann hierarchy is given below, where we now redefine  $\mathbf{x}$  and  $M(\eta)$  to include  $\psi$ , another conformal Newtonian gauge potential:

$$\begin{pmatrix} \dot{\mathbf{x}} \\ \dot{\mathbf{y}} \end{pmatrix} = \begin{pmatrix} M & N \\ O & P \end{pmatrix} \begin{pmatrix} \mathbf{x} \\ \mathbf{y} \end{pmatrix}; \quad (5)$$

$$\mathbf{x} = (\phi, \psi, \delta_r, \delta_m, v_r, v_m); \quad (6)$$

$$\mathbf{y} = (F_{r2}, F_{r3}, \dots); \quad (7)$$

$$M = \begin{pmatrix} 0 & -\mathcal{H} & 0 & 0 & -2H_0^2\Omega_r s^2 & -\frac{3}{2}H_0^2\Omega_m |s| \\ 0 & -\mathcal{H} & 0 & 0 & -\frac{2}{5}H_0^2\Omega_r s^2 & -\frac{3}{2}H_0^2\Omega_m |s| \\ 0 & -4\mathcal{H} & 0 & 0 & -8H_0^2\Omega_r s^2 + \frac{4}{3}k^2 & -6H_0^2\Omega_m |s| \\ 0 & -3\mathcal{H} & 0 & 0 & -6H_0^2\Omega_r s^2 & -\frac{9}{2}H_0^2\Omega_m |s| + k^2 \\ 0 & -1 & -\frac{1}{4} & 0 & 0 & 0 \\ 0 & -1 & 0 & 0 & 0 & -\mathcal{H} \end{pmatrix}; \quad (8)$$

$$N = \begin{pmatrix} 0 & 0 & \dots \\ \frac{6H_0^2\Omega_r \mathcal{H} s^2}{k^2} & \frac{9}{5} \frac{H_0^2\Omega_r s^2}{k} & \dots \\ 0 & 0 & \dots \\ 0 & 0 & \dots \\ \frac{1}{2} & 0 & \dots \\ 0 & 0 & \dots \end{pmatrix}; \quad (9)$$

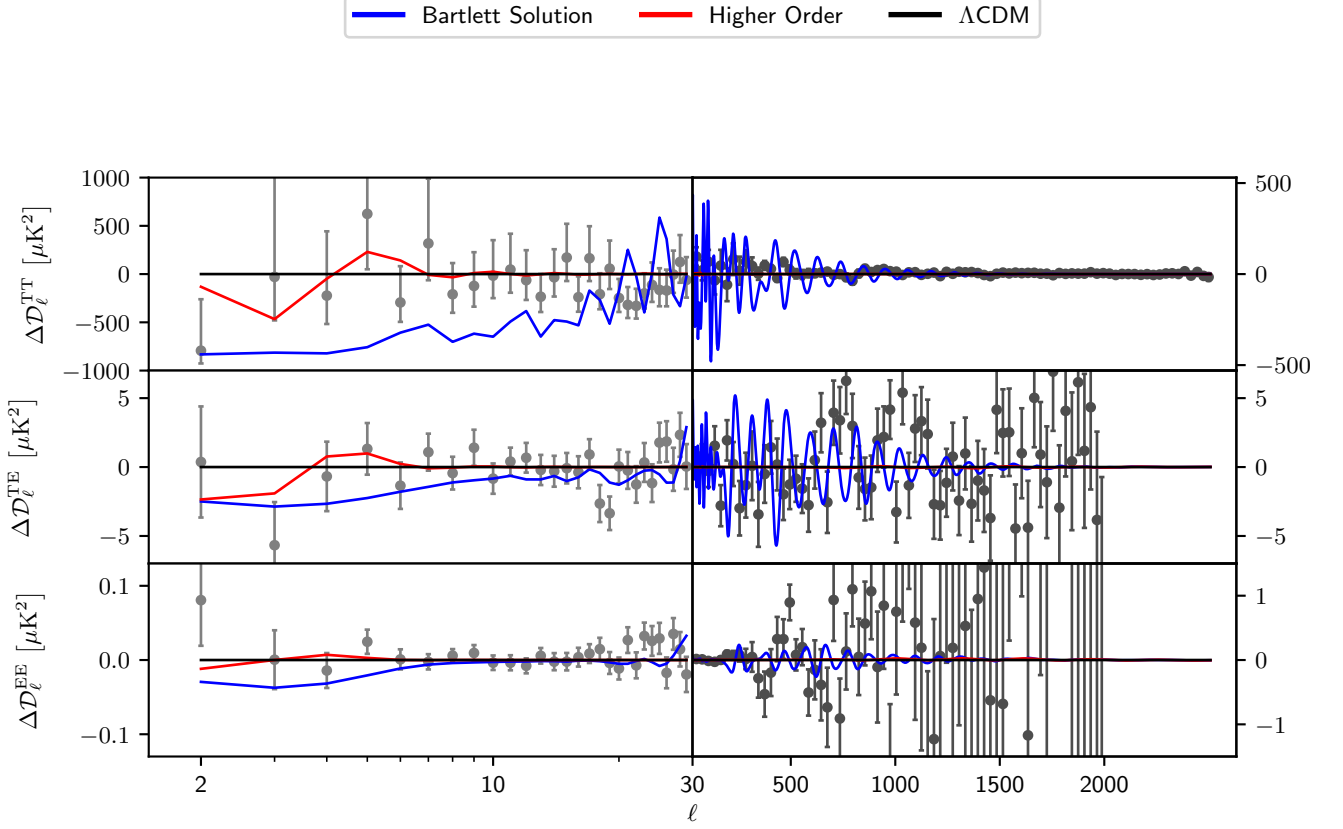


FIG. 1. CMB power spectrum residuals between the quantised model calculated in this paper and the  $\Lambda$ CDM baseline. The corresponding curves for the Bartlett solution (Bartlett *et al.* [2]) are also plotted for reference, as well as Planck residuals. The spectra produced by this new set of  $k$  values appear to be more consistent with the data than the Bartlett solution  $k$  values, but we seem to lose the interesting drop in power at  $\ell \approx 20$  produced in the Bartlett solution. This figure was produced using an adapted version of CLASS [11] used in [2].

$$O = \begin{pmatrix} 0 & 0 & 0 & 0 & -\frac{8}{15}k^2 & 0 \\ 0 & 0 & 0 & 0 & 0 & 0 \\ \vdots & \vdots & \vdots & \vdots & \vdots & \vdots \end{pmatrix}; \quad (10)$$

$$P = \begin{pmatrix} -\frac{9}{10}\frac{n_e\sigma_T}{s} & -\frac{3}{5}k & \cdots \\ \frac{3k}{7} & -\frac{n_e\sigma_T}{s} & \cdots \\ \vdots & \vdots & \ddots \end{pmatrix}, \quad (11)$$

where  $n_e$  is the proper mean density of electrons and  $\sigma_T$  is the Thomson scattering cross-section.

In general, the higher order derivative terms may be written as

$$\dot{F}_{r\ell} = \frac{k}{2\ell+1} [\ell F_{r(\ell-1)} - (\ell+1)F_{r(\ell+1)}] - \frac{n_e\sigma_T}{|s|} F_{r\ell}, \quad (12)$$

where, following [13], when we truncate the equations at

some  $\ell_{\max}$  we set

$$\dot{F}_{r\ell_{\max}} = kF_{r(\ell_{\max}-1)} - \left( \frac{\ell_{\max}+1}{\eta} + \frac{n_e\sigma_T}{|s|} \right) F_{r\ell_{\max}}. \quad (13)$$

The Newtonian gauge potentials can also be written explicitly in terms of the other variables, which will be of use when calculating power series expansions about the Future Conformal Boundary later:

$$\phi = -\frac{3H_0^2}{2k^2} \left( \Omega_m |s| (\delta_m + 3\frac{\dot{s}}{s} v_m) + \Omega_r s^2 (\delta_r + 4\frac{\dot{s}}{s} v_r) \right); \quad (14)$$

$$\psi = \phi - \frac{3H_0^2 \Omega_r}{k^2} s^2 F_{r2}. \quad (15)$$

In this paper we don't solve for  $\phi$  and  $\psi$  explicitly, but this will be discussed further in Section IV A.

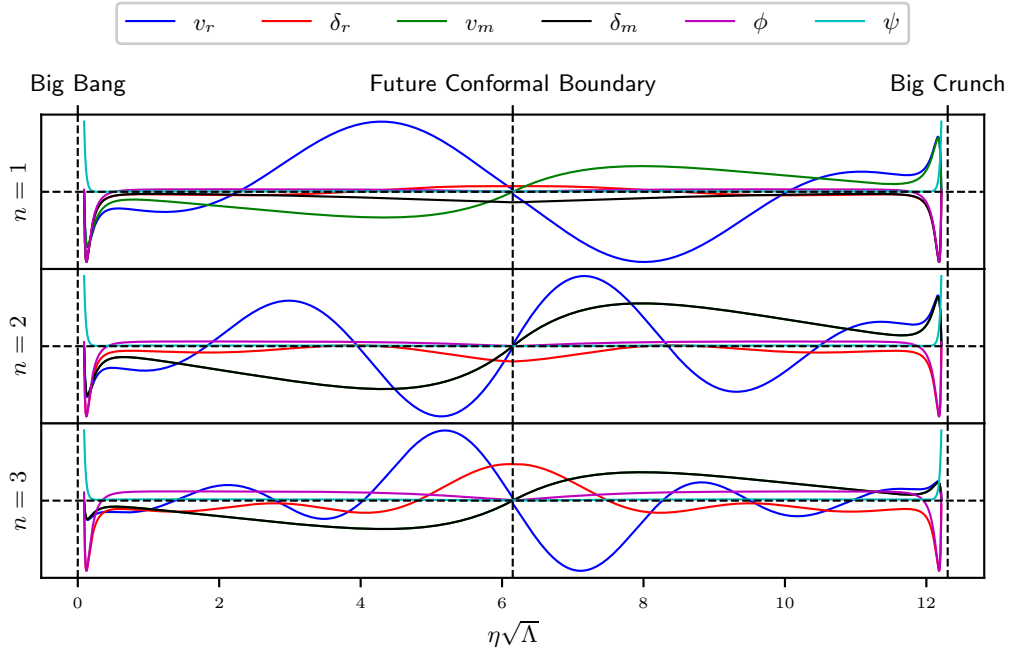


FIG. 2. Base variable solutions are plotted for the first few allowed modes. The solutions become more oscillatory as  $n$  increases.

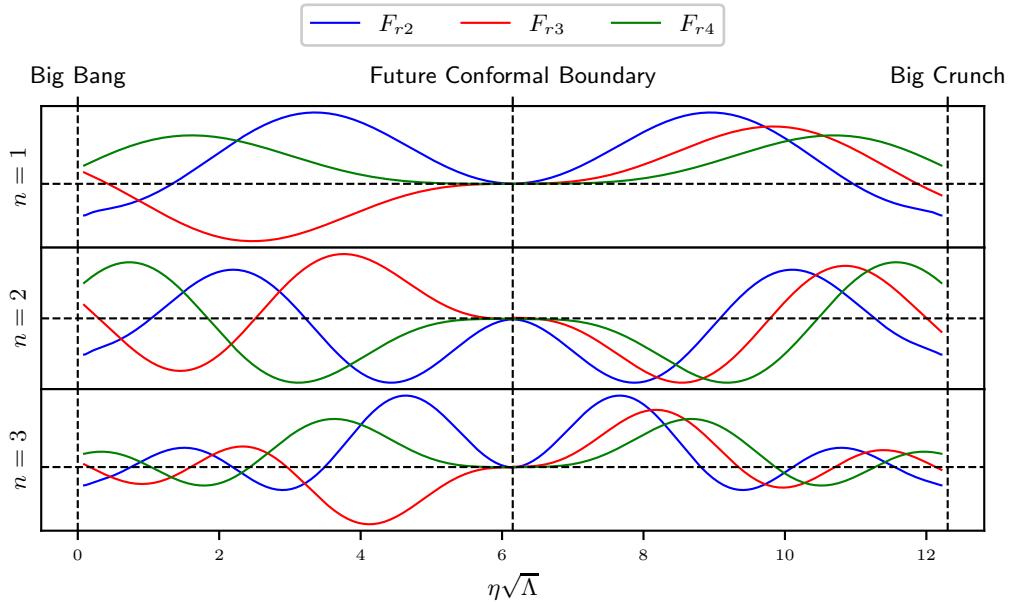


FIG. 3. The first three anisotropic variables are plotted from the end of recombination for the first few allowed modes. We can see that these allowed modes have non-zero recombination values which are  $n$ -dependent.

### C. Imposing Symmetry for Bartlett Case

Below we summarise the argument first discussed in Lasenby *et al.* [1] and then reformulated in Bartlett *et al.* [2] for imposing the quantisation condition  $v_r^\infty = 0$ , where the superscript denotes that the quantity is evaluated at the FCB.

In order to prevent divergence of our solutions at BB2, the first genuine singularity after  $\eta = 0$ , we must impose either symmetry or antisymmetry about the FCB on all of the perturbations. We can see the consequences of this more clearly if we write out the power series expansion of  $\phi$  about the FCB, to linear order:

(such that  $\phi$  is always symmetric about the FCB). This is only satisfied for a discrete set of  $k$  values.

$$\phi = -\frac{3}{2k^2} \left[ \text{sign}(\Delta\eta) \times H_\infty^3 \frac{\Omega_m}{\Omega_\Lambda} (\delta_m^\infty + 3\dot{v}_m^\infty) + 4H_\infty^4 \frac{\Omega_r}{\Omega_\Lambda} v_r^\infty \right] (\Delta\eta) + O(\Delta\eta^3), \quad (16)$$

where  $H_\infty = H_0\sqrt{\Omega_\Lambda}$  is the Hubble constant evaluated at the FCB and  $\Delta\eta$  is the conformal time difference to the actual FCB, defined to be positive before the FCB.

If  $v_r^\infty$  is non-zero, then in order to impose either symmetry or antisymmetry on the above expression we must require that the term depending on the sign of  $\Delta\eta$  is the same either side of the FCB. However, it can be shown that this means we are unable to apply the symmetry condition to  $v_m$  and a contradiction is reached. As such, all valid solutions within this scheme must obey  $v_r^\infty = 0$

---


$$\phi = -\frac{3}{2k^2} \left[ \left( \text{sign}(\Delta\eta) \times H_\infty^3 \frac{\Omega_m}{\Omega_\Lambda} (\delta_m^\infty + 3\dot{v}_m^\infty) + 4H_\infty^4 \frac{\Omega_r}{\Omega_\Lambda} v_r^\infty \right) \Delta\eta + \left( 2H_\infty^4 \frac{\Omega_r}{\Omega_\Lambda} F_{r2}^\infty \right) \Delta\eta^2 + \left( \text{sign}(\Delta\eta) \times \frac{1}{2} H_\infty^3 \frac{\Omega_m}{\Omega_\Lambda} k^2 \dot{v}_m^\infty + H_\infty^4 \frac{\Omega_r}{\Omega_\Lambda} \left( \frac{2}{15} k^2 v_r^\infty - \frac{3}{5} k F_{r3}^\infty \right) \right) \Delta\eta^3 \right] + O(\Delta\eta^4). \quad (17)$$

The key thing here is that if a variable is to be symmetric about the FCB, then the coefficients of odd powers of  $\Delta\eta$  in its power series must swap sign either side of the FCB, such that the product of the coefficient and  $\Delta\eta^n$  (where  $n$  is odd) keeps the same sign on both sides of the boundary. Similarly, its coefficients of even powers of  $\Delta\eta$  must be sign-independent either side of the FCB. The converse must be true for antisymmetric variables.

Let us consider the third term in the  $\phi$  series; in general we will not have  $\dot{v}_m^\infty$  equal to zero. But it is shown in Bartlett *et al.* [2] that enforcing  $v_r^\infty = 0$  results in  $\dot{v}_m^\infty$  being continuous across the FCB and thus keeping the same sign. Hence, this first term of the third-order coefficient keeps  $\phi$  symmetric about the FCB, as required. In order to continue this symmetry we must therefore enforce that the sign-independent term in this expression be zero at the FCB. Since we already have the condition that  $v_r^\infty = 0$  from above, this is equivalent to requiring that  $F_{r3}^\infty = 0$ . We note here that considering the  $\phi$  expansion alone leads to no constraints being placed on  $F_{r2}^\infty$  since the sign-dependent term cancels in the coefficient of  $\Delta\eta^2$ .

After we have enforced the conditions  $v_r^\infty = F_{r3}^\infty = 0$ , we may write the power series expansion of  $F_{r2}$  as

$$F_{r2} = F_{r2}^\infty + k^2 \left[ \frac{1}{15} \delta_r^\infty - \frac{11}{42} F_{r2}^\infty + \frac{6}{35} F_{r4}^\infty \right] \Delta\eta^2 + O(\Delta\eta^3). \quad (18)$$

### III. THEORY

In the following section we calculate the new quantisation conditions at the Future Conformal Boundary which need to be satisfied by the perturbation variables. The key result is given in Section III A.

#### A. Deriving FCB Quantisation Conditions

We may extend the above argument by considering the power series expansion of  $\phi$  up to third order about the FCB when we include higher order terms of the Boltzmann hierarchy. This may be written as

---

Remembering that we require all the variables to be continuous across the FCB, we can see that the effect of  $\delta_r^\infty$  being in general non-zero is that  $F_{r2}$  is forced to be symmetric about the FCB. In fact, it can be shown (see Appendix A) that for every  $F_{r\ell}$  the value of  $\delta_r^\infty$  appears in the coefficient of  $\Delta\eta^\ell$  in the power series. This forces all variables with odd  $\ell$  to be antisymmetric and those with even  $\ell$  to be symmetric about the FCB.

This has profound consequences for the quantisation conditions. If all even modes are required to be symmetric, their first-order derivatives at the FCB must vanish so that the coefficient of  $\Delta\eta$  in their power series will be zero. This is because the first order coefficients can be written entirely in terms of FCB values of higher order variables, which, if not equal to zero at the FCB, are required by continuity to keep the same sign either side of it. But if they keep the same sign, then the overall first-order term will swap sign either side of the FCB, breaking the symmetry requirement. Because of the way the odd and even modes are coupled in the equations, the condition of the first order derivative of even modes disappearing is equivalent to requiring that  $F_{r\ell}^\infty = 0$  for all odd  $\ell$  (see Appendix B for further detail).

Finally, let us consider the coefficient of  $\Delta\eta^3$  in  $F_{r2}$ 's power series. The third order term is where we start to include the Thomson scattering term in the power series. Since  $n_e$  refers to the proper electron density, it is proportional to  $|s|^3$ . Thus the whole Thomson scattering term from Eq. (12) is proportional to  $s^2$  and for clarity

we shall write it as  $Bs^2F_{r\ell}$ , where the constant  $B$  encompasses both the electron density and the Thomson scattering cross-section. In this case the third-order coefficient of  $F_{r2}$ 's series can now be expressed in the form

$$F_{r2}^{(3)} = \frac{8}{45}k^2\phi^{(1)} - \frac{3}{15}kF_{r3}^{(2)} - BH_\infty^2F_{r2}^\infty, \quad (19)$$

where  $\phi^{(1)}$  refers to the coefficient of  $\Delta\eta$  in  $\phi$ 's power series and  $F_{r3}^{(2)}$  refers to the coefficient of  $\Delta\eta^2$  in  $F_{r3}$ 's power series.

Since  $F_{r3}$  is antisymmetric about the FCB, it follows that  $F_{r3}^{(2)}$  at the FCB must either be zero or depend on the sign of  $\Delta\eta$  (in fact, it is zero since all odd  $F_{r\ell}^\infty$  are zero). We recall from Section III A that  $\phi^{(1)}$  also depends on the sign of  $\Delta\eta$ . These both therefore keep  $F_{r2}$  symmetric about the FCB, as required by the arguments above. However, it can be seen that  $F_{r2}^\infty$  must be set to zero if we are to keep this symmetry, since otherwise this term is multiplied by  $\Delta\eta^3$ , which changes sign either side of the FCB.

The third order terms for any even mode,  $n$ , may be written similarly to above, purely in terms of second order odd  $F_{r\ell}$  terms and a term proportional to  $F_{rn}^\infty$ , which can be seen from equation (12). Following the same argument we are forced to set all  $F_{r\ell}^\infty = 0$  for even  $\ell$ .

We thus arrive at our final set of quantisation conditions which are required to enforce the correct symmetry on our equations:

$$\begin{aligned} v_r^\infty &= 0; \\ F_{r\ell}^\infty &= 0 \quad \text{for } \ell \geq 2. \end{aligned} \quad (20)$$

Conversely Lasenby *et al.* [1] and Bartlett *et al.* [2] assume that  $v_r^\infty = 0$ ,  $F_{r\ell}^* = 0$ , where  $*$  refers to the time of recombination — a quite different set of boundary conditions!

## B. Modelling of Recombination

Until recombination we work within the perfect fluid approximation. This means that all higher order terms are set to zero and thus are equal to zero at the start of recombination. In Lasenby *et al.* [1] and Bartlett *et al.* [2], recombination was assumed to be instantaneous: i.e. since we require the variables to be continuous at all conformal times, the higher order terms must be zero at the end of recombination too, at which point we begin solving our Boltzmann hierarchy. If all the higher order terms are initialised to zero at the end of recombination, there will only be one free parameter, the wavenumber,  $k$ , in our set of equations and there is no guarantee of a solution to Section III A.

If, instead of assuming that recombination occurs instantaneously, we consider that it happens over a small finite time so that the higher order modes have time to

grow from zero at the start of recombination to some finite value by the end of recombination, then this introduces additional free parameters into our equations in the form of the exact recombination values of the higher order terms. We will further assume that the effect of this growth on the base variables is negligible, such that the base variables values do not change significantly during recombination.

With this more sophisticated modelling of recombination, we have the same number of free parameters as quantisation conditions, where the final free parameter is  $k$ . Thus we will arrive at a discrete set of  $k$  values for which the quantisation conditions are satisfied, as in Lasenby *et al.* [1] and Bartlett *et al.* [2].

## IV. METHODS

Throughout this paper we use the perfect fluid equations from Section II B 1 before recombination and then assume free-streaming ( $n_e = 0$ ) afterwards; in reality, the Thomson scattering term will be small, hence why we neglect it in this section and assume free-streaming, but it is not actually zero and so must be included when considering boundary conditions. We may calculate the recombination values of base variables by integrating the perfect fluid perturbation equations from  $\eta = 0$  to recombination, using adiabatic initial conditions [1, 2].

### A. General Approach

Since the perturbations can be described by a system of linear differential equations, as in Eq. (5), their solutions form a vector space [16]. This means we are able to encode a linear mapping between solutions at times  $\eta_0$  and  $\eta_1$  using a transfer matrix:

$$x(\eta_1) = U(\eta_1, \eta_0)x(\eta_0). \quad (21)$$

For the case of cosmological perturbations, we may only solve for this transfer matrix numerically, by integrating the perturbation equations between  $\eta_0$  and  $\eta_1$  with initial conditions  $[1,0,0,\dots]$ ,  $[0,1,0,\dots]$  etc. to find each column.

In this case, we are in the somewhat unusual situation of solving a differential equation where some of the variables are specified at one boundary, the time of recombination, and some at the FCB. Since the system is linear, we can solve this without “shooting” methods but, in theory, we still have to integrate either one way or the other in all of the variables in order to obtain the transfer matrix. It makes sense to start the integration at the FCB since we know much more of the variables at this boundary.

So if we now take  $\eta_1 = \eta_*$  to be the conformal time at recombination and  $\eta_0 = \eta_\infty$  to be at the FCB, we can

relate the perturbations at these times similarly using a matrix. Using the same notation for base and anisotropic variables as in Eqs. (6) and (7)), we may write this explicitly as

$$\begin{pmatrix} \mathbf{x}^* \\ \mathbf{y}^* \end{pmatrix} = \begin{pmatrix} A & B \\ C & D \end{pmatrix} \begin{pmatrix} \mathbf{x}^\infty \\ \mathbf{y}^\infty \end{pmatrix}, \quad (22)$$

where the superscript, \*, refers to values at recombination and  $A, B, C, D$  are sub-matrices within the transformation matrix. The values of  $\mathbf{x}^*$  are known from integrating the perfect fluid equations from  $\eta = 0$  to recombination, in the same manner as in Lasenby *et al.* [1] and Bartlett *et al.* [2]. Our modelling of recombination means that the values  $\mathbf{y}^*$  are treated as free parameters and are unknown. On the right-hand side we know what values  $\mathbf{y}^\infty$  should take for the allowed modes, from Section III A, but, apart from  $v_r^\infty, \phi^\infty$  and  $\psi^\infty$ , the values of  $\mathbf{x}^\infty$  are unknowns.

This last point is worth examining more closely: when considering the simultaneous equations produced by the base variables, we see that there will be six equations (from six base variables). But it has also been shown, for example in Section III A, that  $\phi^\infty$  and  $\psi^\infty$  are always equal to zero regardless of  $k$ . This means that there are really only four unknown variables within these six equations. The key thing to note here is Eqs. (14) and (15), which show that both  $\phi$  and  $\psi$  can be determined entirely by the higher order and other base variables and are hence not truly independent variables themselves. So upon closer inspection we see that there is no issue with having six equations describing four unknowns; we may simply discard the top two superfluous equations when solving for the FCB values of the other variables, and we can use Eqs. (14) and (15) to check for consistency.

Going back to Eq. (22), let us explicitly write out the top row:

$$\mathbf{x}^* = A\mathbf{x}^\infty + B\mathbf{y}^\infty. \quad (23)$$

Given that we know we want  $\mathbf{y}^\infty = \mathbf{0}$  in the allowed modes and we know  $\mathbf{x}^*$ , for each  $k$  we can solve for  $\mathbf{x}^\infty$  and then choose the  $k$  values for which  $v_r^\infty = 0$ . This is the general approach we will use to find the allowed wavenumbers. At this stage, we are not interested in the bottom row of Eq. (22) as this doesn't help to solve for  $v_r^\infty$  but can be later used to find the recombination values of higher order terms.

## B. Integrating Backwards from the FCB

In order to obtain the transfer matrix between FCB and recombination values, we must integrate backwards from the FCB using initial conditions of  $[1, 0, 0, \dots], [0, 1, 0, \dots], [0, 0, 1, \dots]$  etc. to find each column of the matrix. This is possible in theory but in practice starting our integration at the exact FCB is highly numerically unstable. Fortunately, it becomes markedly more stable when we start at small deviations from the FCB. Here we have chosen to begin the integration at  $\Delta\eta = 10^{-3}$  before the FCB as this keeps the error in  $v_r^\infty$  relatively small whilst still being close enough to the FCB that we can make efficient use of power series expansions to initialise the variables.

In order to maintain reasonable errors in  $v_r^\infty$ , we must specify the initial conditions up to at least third order in their power series. We must calculate the expansions explicitly for all variables in the hierarchy up to  $\ell = 3$ : for higher order variables we may set the initial condition to zero, where we have used the fact that enforcing the FCB quantisation condition leads to the first non-zero term in the power series of  $F_{r\ell}$  being proportional to  $\Delta\eta^\ell$ .

In order to distinguish those higher order variables which need to be specified at the FCB using power series expansions and those which can simply be set to zero, we now split  $\mathbf{y}$  so that  $\mathbf{y}_{2:4}$  denotes the vector  $[F_{r2}, F_{r3}]$ , and the  $\ell \geq 4$  terms are contained within  $\mathbf{y}_4$ . Using the superscript ' to denote the values of variables at our chosen start point,  $\eta' = \eta_{\text{FCB}} - \Delta\eta$ , we may now rewrite Eq. (22) as

$$\begin{pmatrix} \mathbf{x}^* \\ \mathbf{y}_{2:4}^* \\ \mathbf{y}_4^* \end{pmatrix} = \begin{pmatrix} A & B_{2:4,2:4} & B_{4:,4:} \\ C & D_{2:4,2:4} & D_{4:,4:} \end{pmatrix} \begin{pmatrix} \mathbf{x}' \\ \mathbf{y}_{2:4}' \\ \mathbf{y}_4' \end{pmatrix}, \quad (24)$$

where  $\mathbf{y}_4'$  is  $\mathbf{0}$  and

$$\begin{pmatrix} \mathbf{x}' \\ \mathbf{y}_{2:4}' \end{pmatrix} = \begin{pmatrix} X_1 \\ X_2 \end{pmatrix} \mathbf{X}^\infty. \quad (25)$$

In the above,  $\mathbf{X}^\infty$  represents the vector  $[\delta_r^\infty, \delta_m^\infty, v_r^\infty, \dot{v}_m^\infty]$ . The sub-matrices  $X_1$  and  $X_2$  are given by

$$X_1 = \begin{pmatrix} 0 & -\frac{3}{2k^2}o_m\Delta\eta & o_r(\frac{6}{k^2}\Delta\eta + \frac{1}{5}\Delta\eta^3) & o_m(-\frac{9}{2k^2}\Delta\eta - \frac{3}{4}\Delta\eta^3) \\ 0 & -\frac{2}{k^2}o_m\Delta\eta & o_r(\frac{6}{k^2}\Delta\eta + \frac{1}{5}\Delta\eta^3) & o_m(-\frac{9}{2k^2}\Delta\eta - \frac{3}{4}\Delta\eta^3) \\ 1 - \frac{1}{6}k^2\Delta\eta^2 & o_m(-\frac{6}{k^2}\Delta\eta + \frac{2}{3}\Delta\eta^3) & -\frac{4}{3k^2}(k^4 - 18o_r)\Delta\eta - (\frac{28}{15}o_r - \frac{2}{15}k^4)\Delta\eta^3 & o_m(-\frac{18}{k^2}\Delta\eta - \Delta\eta^3) \\ 0 & 1 + o_m(-\frac{9}{2k^2}\Delta\eta + \frac{1}{2}\Delta\eta^3) & o_r(\frac{18}{k^2}\Delta\eta - \frac{1}{5}\Delta\eta^3) & \frac{1}{2}k^2\Delta\eta^2 - o_m(\frac{27}{2k^2}\Delta\eta + \frac{3}{4}\Delta\eta^3) \\ \frac{1}{4}\Delta\eta - \frac{1}{40}k^2\Delta\eta^3 & -\frac{2}{2k^2}o_m\Delta\eta^2 & 1 + \frac{1}{k^2}(6o_r - \frac{3}{10}k^4\Delta\eta^2) & -\frac{9}{2k^2}o_m\Delta\eta^2 \\ 0 & -\frac{3}{2k^2}o_m\Delta\eta^2 & \frac{6}{k^2}o_r\Delta\eta^2 & -\Delta\eta - \frac{9}{2k^2}o_m\Delta\eta^2 \end{pmatrix}; \quad (26)$$

$$X_2 = \begin{pmatrix} \frac{1}{15}k^2\Delta\eta^2 & -\frac{4}{15}o_m\Delta\eta^3 & \frac{8}{15}k^2\Delta\eta - \frac{16}{15}(\frac{1}{14}k^4 - o_r)\Delta\eta^3 & -\frac{4}{5}o_m\Delta\eta^3 \\ -\frac{1}{105}k^3\Delta\eta^3 & 0 & -\frac{4}{35}k^3\Delta\eta^2 & 0 \end{pmatrix}, \quad (27)$$

Parameter	TT+lowE 68% limits
$\Omega_\Lambda$	0.679
$\Omega_m$	0.321
$\Omega_r$	$9.24 \times 10^{-5}$
$H_0$	0.701
$z^*$	1090.30

TABLE I. Planck best-fit values from [4], after being re-scaled to new units of  $8\pi G = c = \hbar = \Lambda = 1$ .

where  $o_m = H_\infty^3 \frac{\Omega_m}{\Omega_\Lambda}$  and  $o_r = H_\infty^4 \frac{\Omega_r}{\Omega_\Lambda}$  are reduced matter and radiation parameters, and simply contain the coefficients of the power series expansions for the base,  $F_{r2}$  and  $F_{r3}$  variables.

Writing out the top row of Eq. (24) as

$$\mathbf{x}^* = (AX_1 + B_{2:4,2:4}X_2)\mathbf{X}^\infty + B_{4:,4:}\mathbf{0}, \quad (28)$$

we see a major simplification to the problem: given that the matrix  $B_{4:,4:}$  is always going to be multiplied by the zero vector, there is no need to find its components explicitly. We are thus able to greatly reduce our computation time by only having to perform eight integrations to determine the first eight columns of each transfer matrix (six for the base variables and two more for  $F_{r2}$  and  $F_{r3}$ ), and we can set the remaining columns to zero. This is especially useful given that we are unable to use traditional time-saving approximations used in Boltzmann codes, such as estimating the higher order terms using spherical Bessel functions [11], when we get close to the FCB.

### C. Implementation of Code

Throughout the code we work with dimensionless units for the comoving wavenumber by writing  $k = K\sqrt{\Lambda}$ . We also choose units such that  $\sqrt{\Lambda}$  is unity, so we may write the present-day Hubble value as  $H_0 = \frac{1}{3\Omega_\Lambda}$ . All relevant  $\Lambda$ CDM parameters are taken from the Planck best-fit values, given in the posterior samples TT+lowE [4]. The re-scaled values are given in Table I.

For each value of  $K$  between 0 and 20, the background and perturbation equations were integrated, using the necessary initial conditions, from

the FCB to recombination using LSODA from `scipy.integrate.solve_ivp`. Once the transfer matrix was obtained in this way, Eq. (28) was set up and solved using `numpy.linalg.solve` to find the value of  $v_r^\infty$ . This was then plotted against  $K$  and the allowed modes were determined by finding where this curve intersected the  $x$ -axis.

## V. RESULTS AND DISCUSSION

### A. Final Allowed Modes

The final, converged, graph of  $v_r^\infty$  against  $K$  is presented in Fig. 4, with  $\ell_{max} = 70$ , a choice which will be justified in the following section; the corresponding curve for the Bartlett solution is included for a direct comparison. Qualitatively, we can see that the allowed modes, when higher order terms of the Boltzmann hierarchy are included, are more closely spaced than in the Bartlett solution. As in Lasenby *et al.* [1] and Bartlett *et al.* [2], although the spacing of the modes is initially non-linear, it settles down to linear fairly quickly, as shown in Fig. 5.

This linear spacing, as well as the lowest allowed wavenumber, is:

$$k_0 = 0.309\sqrt{\Lambda} = 9.93 \times 10^{-5}\text{Mpc}^{-1} \quad (29)$$

$$k_1 = 1.328\sqrt{\Lambda} = 4.27 \times 10^{-3}\text{Mpc}^{-1} \quad (30)$$

$$\Delta k = 0.507\sqrt{\Lambda} = 1.63 \times 10^{-4}\text{Mpc}^{-1}. \quad (31)$$

For reference, the equivalent values for the Bartlett imperfect fluids solution are [2]:

$$k_0^{\text{Bartlett}} = 0.042\sqrt{\Lambda} = 1.34 \times 10^{-5}\text{Mpc}^{-1} \quad (32)$$

$$k_1^{\text{Bartlett}} = 5.39\sqrt{\Lambda} = 1.73 \times 10^{-3}\text{Mpc}^{-1} \quad (33)$$

$$\Delta k^{\text{Bartlett}} = 0.657\sqrt{\Lambda} = 2.11 \times 10^{-4}\text{Mpc}^{-1}. \quad (34)$$

A key difference between the two curves in Fig. 4 is that the second allowed mode occurs at a much smaller  $K$  value ( $K = 1.33$ , as opposed to 5.39) and the ‘‘missing modes’’ from the Bartlett solution are re-introduced. In fact, these modes are re-introduced even for the case where we consider the  $\ell = 2$  terms, if we take  $F_{r2}$  as a free parameter. The other difference is that the new spacing between the allowed modes is smaller. The first few allowed modes are plotted in Figs. 2 and 3.



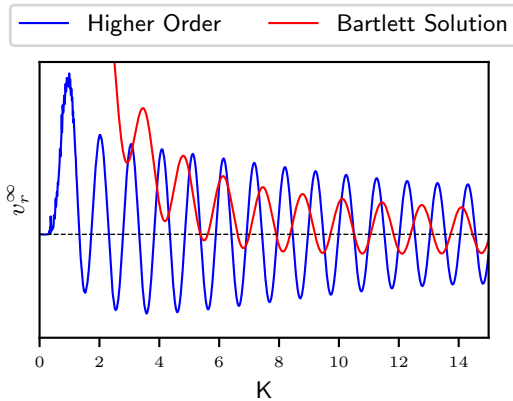


FIG. 4. Converged values of  $v_r^\infty$ , solved using the method described in Section IV, are plotted as a function of the dimensionless comoving wavenumber  $K$ . The equivalent curve for the Bartlett solution [2] is also plotted for reference.

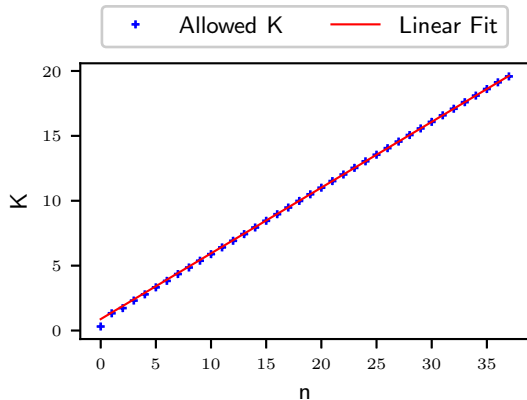


FIG. 5. The first 38 allowed wavenumbers have been explicitly calculated and plotted. It is clear from the excellent agreement of the linear fit that the spacing between the allowed  $K$  values quickly settles down to a constant.

## B. Convergence of Allowed Modes

We can examine the degree of convergence of solutions by taking several different values of  $\ell_{\max}$ , the order at which the Boltzmann hierarchy is truncated, and plot the curves of  $v_r^\infty$  against  $K$  for each of these to see how changing  $\ell_{\max}$  shifts the allowed modes. This is demonstrated in Fig. 6, which will be discussed further in the following section.

In fact, the results show a remarkable convergence of the curves, even at relatively low values of  $\ell_{\max}$ , indicating that the transition from the Bartlett case is due to just a few critical low- $\ell$  modes.

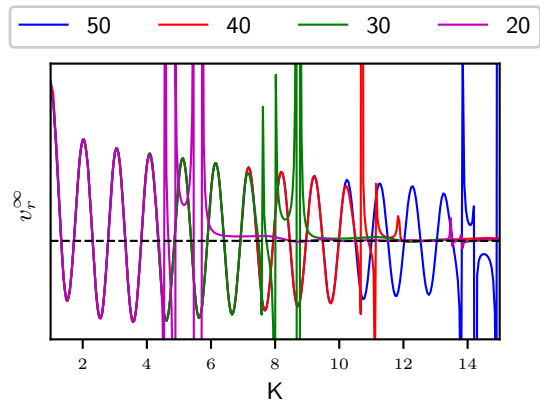


FIG. 6.  $v_r^\infty$  is plotted as a function of  $K$  for various values of  $\ell_{\max}$ , the order at which our Boltzmann hierarchy is truncated. For values of  $\ell_{\max}/K \lesssim 4$ , the curves begin to misbehave, potentially due to unphysical reflection as warned in [11].

## C. Truncation and Artificial Reflection

We must truncate our Boltzmann hierarchy at some  $\ell_{\max}$ , and a smaller  $\ell_{\max}$  leads to a less computationally-expensive code. However, truncating too early leads to some unexpected behaviour of our graphs, and the regular oscillating behaviour of  $v_r^\infty$  in  $K$ -space is lost. This is likely due to artificial reflection of power from  $\ell_{\max}$  back to lower multipoles, as suggested in [11]. Although the alternative truncation scheme quoted in Eq. (13), proposed in [13], is designed to minimise this, significant levels of unphysical reflection cannot be avoided for late times. The value of  $\ell_{\max}$  should thus scale with  $k\eta$ .

In order to demonstrate the effect of truncation, graphs of  $v_r^\infty$  against  $K$  have been plotted for  $\ell_{\max} = 20, 30, 40$  and 50. As can be seen in Fig. 6, the graphs begin to deviate from their regular structure at  $\ell_{\max}/K \approx 4$ . It is interesting to note, however, that before the graphs begin to diverge, they still give the same allowed modes; this again reinforces that the transition to these new allowed modes is likely due to just a few critical low- $\ell$  modes.

## D. The Choice of Root Finding Variable

It should be noted that, although in this paper we have chosen to search for zeros in  $v_r^\infty$  to determine the allowed modes, this decision is largely arbitrary. Since it does not matter in which order we solve the quantisation conditions, we could in theory set  $v_r^\infty$  to zero initially and then search for zeros in any of the other higher order multipoles. These will all lead to the same allowed modes, and all have the same issue of artificial reflection of power for too small  $\ell_{\max}$  so, numerically-speaking, there is no clear advantage to any. One advantage of looking for zeros in  $v_r^\infty$  is that it is more directly comparable to the work

in Lasenby *et al.* [1] and Bartlett *et al.* [2].

We could also start by setting  $v_r^\infty$  to zero as well, use three of the four base variable equations to solve for the remaining three FCB values and then use the fourth equation to match onto the recombination value of the fourth variable. Again, this is of a similar stability to the other methods provided we do not truncate the equations too early.

### E. Discussion of $k_0$ and $\Delta k$

We may use the calculated values of  $k_0$  and  $\Delta k$  from Section V A to compute a  $C_\ell$  power spectrum and compare this with observational data. However, in Bartlett *et al.* [2] the general class of linearly quantised models was assessed so we may use these for an initial comparison of our values.

In Figures 5 and 8 of Bartlett *et al.* [2], likelihood plots showing the difference in quality of fit between the linearly quantised models and  $\Lambda$ CDM models are given, as functions of  $k_0$  and  $\Delta k$ . Qualitatively, it appears that the linearly quantised model calculated in this project gives roughly the same quality of fit as the  $\Lambda$ CDM model. However, it is important to note that the models in Bartlett *et al.* [2] were examined using a profile likelihood analysis. Gessey-Jones and Handley [17] have shown that the conclusions may change if investigated using a Bayesian approach, although more work is required to test the full suite of predictions against matter power spectrum constraints.

Figure 1 shows the CMB power spectrum residuals between the quantised model found in this project and the  $\Lambda$ CDM baseline, produced using the code from Bartlett *et al.* [2] which is an adapted version of CLASS [11]. It can be seen that the resulting spectra in this case appear to be more consistent with cosmological data than the Bartlett solution, but it is interesting to see that we lose some of the noteworthy low- $\ell$  features of the latter, such as the dip in power at  $20 \lesssim \ell \lesssim 30$ . The spectra shown in Fig. 1 should be interpreted with some caveats as for a fair comparison we ought to explicitly calculate within a discrete model the  $C_\ell$  power spectrum arising from this quantisation; indeed, this leaves the possibility that the quantised model may even provide a better fit to the data than the  $\Lambda$ CDM baseline.

## VI. CONCLUSION

We have extended the results of Lasenby *et al.* [1] and Bartlett *et al.* [2] to include higher order terms of the Boltzmann hierarchy in calculating the quantised spectrum of comoving wavenumbers for a palindromic universe containing radiation, dark matter and a cosmological constant. We derived a new set of quantisation conditions needed to impose the correct symmetry on the solutions to the cosmological perturbation equations,

such that they do not diverge at the singularity after the Future Conformal Boundary. A more sophisticated modelling of the evolution of perturbations through recombination has been employed to enable a consistent set of solutions to these quantisation conditions. Using this, the discrete set of comoving wavenumbers satisfying these conditions were calculated by exploiting the linear nature of the equations.

The lowest permissible wavenumber within this model was calculated to be  $k_0 = 9.93 \times 10^{-5} \text{Mpc}^{-1}$  and allowed modes are separated by a linear spacing of  $\Delta k = 1.63 \times 10^{-4} \text{Mpc}^{-1}$ . An initial comparison of these values to the general class of linearly quantised models considered in Bartlett *et al.* [2] indicate that the spectra produced from this quantisation are fairly consistent with observational data. However, the  $C_\ell$  power spectrum must be explicitly calculated within a discrete model in order to fairly assess the quality of agreement of this model with observed data.

The spacing of these allowed modes ceases to change upon addition of further higher order terms at a relatively low value of  $\ell_{\text{max}}$ , indicating that the transition from the Bartlett solution occurs due to just a few critical low- $\ell$  modes.

In addition to computing the  $C_\ell$  spectrum, further work could explore a more detailed modelling of recombination, as well as including the Thomson scattering term in the integration of variables. A Bayesian analysis could also be performed on the general class of linearly quantised models in order to obtain updated fits for  $(k_0, \Delta k)$  values. One of the main limitations of the methods described in this paper is the long run-time of the code to solve the Boltzmann hierarchy at large  $k$  values, due to the highly oscillatory nature of the solutions. More efficient methods have recently been developed to solve differential equations with rapidly oscillating solutions, such as the RKWKB method for one-dimensional systems [18] and Magnus expansion based methods for higher-dimensional ones [14], but more work needs to be done before the use of these can be extended up to high  $\ell$  values. A recent paper [19] has explored an alternative formulation of the perturbation equations, whereby the Boltzmann hierarchy is replaced by just two integral equations describing the photon intensity quadrupole and the linear-polarisation quadrupole, and such techniques could prove more numerically suitable when executing a full pipeline confronting these models of the Universe against the latest cosmological data.

## ACKNOWLEDGMENTS

We thank Deaglan Bartlett for helpful conversations about his work on this subject. MP thanks the Cavendish Laboratory for the Part III Project opportunity. WH is supported by a Royal Society University Research Fellowship.

### Appendix A:

Below we argue that  $\delta_r^\infty$  always appears in the coefficient of  $\Delta\eta^\ell$  in the power series expansions of higher order variables about the FCB. This is used in section III A to argue that all variables with odd  $\ell$  are forced to be antisymmetric about the FCB, and all variables with even  $\ell$  are forced to be symmetric.

The power series expansion about the FCB for a higher order variable may be written in general as:

$$F_{r\ell} = F_{r\ell}^\infty + \dot{F}_{r\ell}^\infty \Delta\eta + \frac{1}{2} \ddot{F}_{r\ell}^\infty \Delta\eta^2 + \dots \quad (\text{A1})$$

$$+ \frac{1}{n!} F_{r\ell}^{(n)\infty} \Delta\eta^n + \dots \quad (\text{A2})$$

Now,  $\dot{F}_{r\ell}$  will depend on  $F_{r(\ell-1)}$ ,  $F_{r\ell}$  and  $F_{r(\ell+1)}$  only (from equation (12)). Let's consider the coefficient of  $\Delta\eta^\ell$  in the above power series:

$F_{r\ell}^{(\ell)}$  will depend on  $F_{r(\ell-1)}^{(\ell-1)}$ ,  $F_{r(\ell)}^{(\ell-1)}$  and  $F_{r(\ell+1)}^{(\ell-1)}$  only. But, for example,  $F_{r(\ell-1)}^{(\ell-1)}$  will depend on  $F_{r(\ell-2)}^{(\ell-2)}$ ,  $F_{r(\ell-1)}^{(\ell-2)}$  and  $F_{r(\ell)}^{(\ell-2)}$ . If we keep following this through until we express the coefficient in terms of just the higher order variables themselves (as opposed to derivatives of them), then eventually  $\dot{v}_r^\infty$  will be used, which depends on  $\delta_r^\infty$ . This is the smallest coefficient for which  $\delta_r^\infty$  appears as for the coefficient of  $\Delta\eta^{(\ell-1)}$ , if we express this just in terms of the higher order variables, the first term will be

proportional to  $v_r^\infty$ , and for the coefficient of  $\Delta\eta^{(\ell-2)}$  the first term will be proportional to  $F_{r2}^\infty$  and so on.

### Appendix B:

Here we show that requiring the first order derivatives of even  $\ell$  terms to disappear is equivalent to requiring that  $F_{r\ell} = 0$  for all odd  $\ell$ . The first order derivative of an even  $\ell$  variable may be written as:

$$\dot{F}_{r\ell} = \frac{k}{2\ell+1} [\ell F_{r(\ell-1)} - (\ell+1)F_{r(\ell+1)}] - Bs^2 F_{r\ell}, \quad (\text{B1})$$

from equation (12) and from section III A where we write the Thomson term as being proportional to  $s^2$ . However, in the power series solution,  $s$  must be written as a power series expansion about the FCB too;  $s$  can be written as  $H_\infty \Delta\eta + \dots$  so in the first order power series term,  $\dot{F}_{r\ell} \Delta\eta$ , the Thomson term is in fact proportional to  $\Delta\eta^3$  and is thus not first order. So to first order in  $\Delta\eta$ , we only have  $\frac{k}{2\ell+1} [\ell F_{r(\ell-1)} - (\ell+1)F_{r(\ell+1)}]$  as the coefficient to  $\Delta\eta$ . So requiring that this coefficient disappears is equivalent to requiring that  $\ell F_{r(\ell-1)} = (\ell+1)F_{r(\ell+1)}$  for all even  $\ell$ .

Let's start from  $\ell = 4$ : since we have already enforced  $F_{r3}^\infty = 0$  earlier on in the argument in section III A, this means that  $F_{r5}^\infty$  is now also forced to be zero. Similarly, for  $\ell = 6$ , since  $F_{r5}^\infty$  has been forced to be zero,  $F_{r7}^\infty$  is now also forced to be zero, and so on. Thus, for all odd  $\ell$  we require that  $F_{r\ell}^\infty$  be zero.

- 
- [1] A. N. Lasenby, W. J. Handley, D. J. Bartlett, and C. S. Negreanu, "Perturbations and the future conformal boundary," (2021), arXiv:2104.02521 [gr-qc].
  - [2] D. J. Bartlett, W. J. Handley, and A. N. Lasenby, "Improved cosmological fits with quantized primordial power spectra," (2021), arXiv:2104.01938 [astro-ph.CO].
  - [3] S. Perlmutter, G. Aldering, G. Goldhaber, R. A. Knop, P. Nugent, P. G. Castro, S. Deustua, S. Fabbro, A. Goobar, D. E. Groom, and et al., *The Astrophysical Journal* **517**, 565–586 (1999).
  - [4] N. Aghanim, Y. Akrami, M. Ashdown, J. Aumont, C. Baccigalupi, M. Ballardini, A. J. Banday, R. B. Barreiro, N. Bartolo, and et al., *Astronomy & Astrophysics* **641**, A6 (2020).
  - [5] L. Boyle and N. Turok, "Two-sheeted universe, analyticity and the arrow of time," (2021), arXiv:2109.06204 [hep-th].
  - [6] Planck Collaboration, *A&A* **641**, A5 (2020).
  - [7] C. J. Copi, D. Huterer, D. J. Schwarz, and G. D. Starkman, *Monthly Notices of the Royal Astronomical Society* **367**, 79–102 (2006).
  - [8] C. J. Copi, D. Huterer, D. J. Schwarz, and G. D. Starkman, *Advances in Astronomy* **2010**, 1–17 (2010).
  - [9] A. Rassat, J. L. Starck, P. Paykari, F. Sureau, and J. Bobin, *Journal of Cosmology and Astroparticle Physics* **2014** (2014), 10.1088/1475-7516/2014/08/006.
  - [10] M. R. Gangopadhyay, G. J. Mathews, K. Ichiki, and T. Kajino, *The European Physical Journal C* **78** (2018), 10.1140/epjc/s10052-018-6218-x.
  - [11] D. Blas, J. Lesgourgues, and T. Tram, *Journal of Cosmology and Astroparticle Physics* **2011**, 034–034 (2011).
  - [12] M. P. Hobson, G. P. Efstathiou, and A. N. Lasenby, *General Relativity: An Introduction for Physicists* (Cambridge University Press, 2006).
  - [13] C.-P. Ma and E. Bertschinger, *The Astrophysical Journal* **455**, 7 (1995).
  - [14] J. Bamber and W. Handley, *Physical Review D* **101** (2020), 10.1103/physrevd.101.043517.
  - [15] S. Dodelson, *Modern Cosmology* (Academic Press, Elsevier Science, 2003).
  - [16] S. Lang, *Algebra* (Springer, New York, NY, 2002).
  - [17] T. Gessey-Jones and W. J. Handley, *Phys. Rev. D* **104**, 063532 (2021), arXiv:2104.03016 [astro-ph.CO].
  - [18] F. J. Agocs, W. J. Handley, A. N. Lasenby, and M. P. Hobson, *Physical Review Research* **2** (2020), 10.1103/physrevresearch.2.013030.
  - [19] M. Kamionkowski, "Cosmological perturbations without the boltzmann hierarchy," (2021), arXiv:2105.02887 [astro-ph.CO].